MOLECULAR AND CELLULAR BIOLOGY, Aug. 1988, p. 3094–3103
0270-7306/88/083094-10$02.00/0

Vol. 8, No. 8

A Dominant Trifluoperazine Resistance Gene from *Saccharomyces cerevisiae* Has Homology with F_0F_1 ATP Synthase and Confers Calcium-Sensitive Growth

CHENG-KON SHIH, RONALD WAGNER, SABINE FEINSTEIN, CYNTHIA KANIK-ENNULAT, AND NORMA NEFF*

Graduate Program in Molecular Biology, Memorial Sloan-Kettering Cancer Center, 1275 York Avenue, New York, New York 10021

Received 9 November 1987/Accepted 20 April 1988

The antipsychotic drug trifluoperazine has been long considered a calmodulin inhibitor from in vitro studies but may function in vivo as a more general inhibitor by disturbing ion fluxes and altering the membrane potential. Resistance to trifluoperazine can arise in *Saccharomyces cerevisiae* cells by alterations in at least three distinct genetic loci. One locus, defined by a spontaneous dominant trifluoperazine resistance mutation (*TFP1-408*), was isolated and sequenced. The sequence of the *TFP1-408* gene revealed a large open reading frame coding for a large protein of 1,031 amino acids with predicted hydrophobic transmembrane domains. A search of existing amino acid sequences revealed a significant homology with F_0F_1 ATP synthase. Mutant *TFP1-408* cells did not grow efficiently in the presence of 50 mM $CaCl_2$, whereas wild-type cells did. Wild-type cells became resistant to trifluoperazine in the presence of 50 mM $CaCl_2$ or 50 mM $MgCl_2$. Mutant cells showed a higher rate of calcium transport relative to wild-type cells. These data suggest that the *TFP1* gene product codes for a transmembrane ATPase-like enzyme possibly involved in Ca^{2+} transport or in generating a transmembrane ion gradient between two cellular compartments.

The mechanism of action of the phenothiazine tranquilizers has been the subject of numerous studies (42). Studies reported in the pharmacological literature suggest that the phenothiazines inhibit one of the two types of dopamine receptors (24, 48), a hypothesis consistent with the antipsychotic and Parkinson's disease-like effects. Reports in the biochemical literature suggest that the phenothiazines may function as inhibitors of calcium-binding proteins, especially calmodulin (50) and protein kinase C (25), and may affect calcium- or calmodulin-regulated processes in cells (47). This alternative model is consistent with the effect of these drugs in vivo, since neurons and muscle cells are two types of cells in the body that are dependent on calcium gradients or currents for function.

The medical effectiveness of the phenothiazines is directly related to the hydrophobicity of the molecule and varies with the side-chain modifications to the planar ring (50). Trifluoperazine (TFP) is the most hydrophobic of the medically effective phenothiazines. The hydrophobic character of the phenothiazine tranquilizers confers two properties to the drugs: lipid solubility and membrane association. Therefore these drugs can cross the blood-brain barrier readily, can get into any cell type, and can associate with or intercalate into any membranous structure.

Since TFP is a medically important drug that affects cells that are dependent upon calcium gradients for function in vivo and inhibits calcium-binding proteins with hydrophobic domains in vitro, we isolated spontaneous TFP-resistant mutants of the simple eucaryote *Saccharomyces cerevisiae* in an attempt to find mutations in genes coding for proteins involved in calcium transport or regulated pathways. Calcium-sensitive or -dependent mutants of *S. cerevisiae* have been isolated before (30–32), and calcium-related biochemical activities have been documented in *S. cerevisiae* (8, 10–12, 29, 38). TFP-resistant pseudorevertants of a calcium-dependent mutation have been isolated and are recessive to the wild type for TFP resistance and show TFP-dependent growth at 37°C (30). In this report we describe the isolation and characterization of a spontaneous mutation to dominant TFP resistance and the sequence of the gene encoding it.

* Corresponding author.

MATERIALS AND METHODS

Strains and plasmids. *S. cerevisiae* strains were of the S288c background. The wild-type haploids used in this work were NF134 (*Mata his4-539 lys2-801 ura3-52*) and NF147 (*MATα ade2-101 ura3-52*) (43). NF408 was a spontaneous mutation of NF147 to dominant TFP resistance. Bacterial strains and yeast plasmid vectors were as described previously (27, 43). Plasmids containing the *HO*, *CDC7*, and *TRT1* genes were provided by Mary Ann Osley. The translocation strain YNN311 was constructed and provided by Michael Fasullo (Ph.D. thesis, Stanford University, Palo Alto, Calif., 1985). This strain contained a translocation of chromosome II (*GAL1*, *GAL10*, *GAL7*, and *CEN2*, and left arm) to the right arm of chromosome IV (beginning at *TRP1*), and the left arm of chromosome IV plus *CEN4* to the right arm of chromosome II (near the *GAL1*, *GAL10*, and *GAL7* locus).

Preparation and storage of TFP media. Stock solutions of TFP (gift from Smith Kline and French) were prepared in sterile water in dim light and stored at −20°C in the dark. A molar extinction coefficient of log ε 4.50 at 258 nm was used (33). YPD plates (45) containing TFP were made frequently and stored and incubated in the dark. Phenotype was scored with a metal-pronged replicator (Watson Products) and disposable plastic microdilution wells. Conventional replica plating with velvet transferred too many cells and was not reproducible.

Yeast media, genetic methods, and growth efficiency study. Standard yeast media and tetrad analysis were as described

by Sherman et al. (45). Spontaneous mutants to TFP resistance were isolated by spreading colonies of NF134 and NF147 cells on YPD plates containing 10 to 15 μM TFP and incubating the plates at 26°C for 3 days. To test growth efficiency, cell cultures with an A_{600} of 0.4 (2×10^7 to 3×10^7 cells per ml) were diluted 1:10 into test media with or without 1 to 50 μM TFP. The cultures were grown overnight (14 to 16 h) in the dark, and the A_{600} of the cultures was measured. The absorbance of the culture was recorded directly when the reading was less than 1. Cultures of higher absorbance were diluted with YPD (generally 1:50) before measurement. Wild-type and mutant cells grew routinely to an A_{600} of 15 (2×10^8 cells per ml) under permissive conditions. Growth efficiency is expressed as the percentage of cell growth in test condition medium relative to that of cells in permissive condition medium in each experiment.

^{45}Ca uptake. Uptake experiments were performed as described by Eilam (10, 11) with minor modifications. $^{45}Ca^{2+}$ was purchased from New England Nuclear Corp. Freshly grown log-phase cells (A_{600} of 0.3 to 1.0) were stored on ice for 1 to 2 h until needed. The YPD cultures were harvested, washed once with water, and suspended in 20 mM 2-*N*-morpholinoethane sulfonic acid (MES)–Tris buffer (pH 6.0) with 2% glucose at a density of 2×10^7 cells per ml. The cells were diluted at time zero with an equal volume of MES-Tris buffer and 2% glucose plus a defined concentration of $^{45}CaCl_2$ (specific activity, 12 to 10^4 cpm/pmol; concentration, 2 μM to 20 mM). Samples were removed at specific time intervals (1 to 60 min), diluted with 8 volumes of cold 20 mM $MgCl_2$, and immediately filtered.

Recombinant DNA methods, chromosome separation gels, and DNA sequence analysis. Recombinant DNA methods (phage growth, ligations, plasmid isolation, gel transfer-hybridization, and DNA fragment size fractionation) were those of Maniatis et al. (22) and Davis et al. (7).

Genomic DNA was made from NF408 cells (16, 45) and partially digested with the restriction enzyme *Sau*3A. The DNA fragments were fractionated by size on a sucrose gradient, and the 10- to 20-kilobase (kb) size class was pooled and ligated into the yeast plasmid vector YCp50. Twenty-five thousand individual ampicillin-resistant, tetracycline-susceptible colonies resulting from the transformation of the ligation mixture into *Escherichia coli* were pooled, and plasmid DNA was prepared. This plasmid pool of random NF408 genomic DNA fragments was transformed into NF134 cells, and URA^+ transformants were selected. Plasmid DNA was transformed into yeast cells treated with lithium acetate by the method of Ito et al. (17) with the addition of 50 to 100 μg of sheared *E. coli* DNA as the carrier. Ten thousand URA^+ yeast colonies were pooled, and dilutions of the transformant cells were plated onto YPD plates with 12.5 μM TFP to select for cells containing the dominant TFP resistance gene.

Genomic DNA from NF134 was partially digested with restriction enzyme *Sau*3A, and 15- to 20-kb fragments were ligated into the lambda cloning vector EMBL3B (18, 22), creating a library of wild-type sequences.

Yeast chromosome separation was performed as described by Carle and Olsen (4) with a contour-clamped homogeneous electric field gel apparatus (5).

The 5-kb *Bam*HI-to-*Xba*I fragment (see Fig. 3) containing the *TFP1-408* gene was cloned into the single-stranded M13 phage vector M13mp9 (23), and deletions were generated from clones of both orientations by the method of Dale et al. (6). DNA sequence was determined by the dideoxy-chain termination method of Sanger et al. (40) with modifications by Barnes et al. (2).

Gene disruption by insertion and null allele replacement constructions. The 1.8-kb *Eco*RI restriction fragment, which is entirely within the coding region of the *TFP1* gene (see Fig. 3), was ligated into the *Eco*RI site of the yeast integrating vector YIp5. The resulting plasmid (pTFP1-18) contained a unique *Kpn*I restriction enzyme site within the *TFP1* sequence and a unique *Sma*I restriction enzyme site with the *URA3* sequence. These unique restriction enzyme sites were used to linearize the plasmid to direct its integration to either the *TFP1* or *URA3* locus (36). The linearized pTFP1-18 DNA was transformed into a haploid strain (NF147) or into a diploid strain (NF408 × NF134), and URA^+ transformants were selected.

The null allele was constructed by digesting the 5.5-kb *Xba*I fragment with restriction enzymes *Eco*RV and *Cla*I (see Fig. 3), which removes the entire open reading frame, and replacing it with the 1.1-kb $URA3^+$ *Hin*dIII fragment by a blunt-end ligation reaction. The pUC12 plasmid vector (23) DNA containing the null construction (pTFP1-13) was digested with *Xba*I and transformed into a wild-type diploid of NF134 × NF147, and URA^+ colonies were selected (36).

RESULTS

Isolation of TFP-resistant mutants. Spontaneous mutants resistant to 10 to 15 μM TFP were found at the frequency of 1 in 10^7 cells in *S. cerevisiae*. Two-thirds of the spontaneous TFP-resistant mutants were recessive to the wild type for drug resistance. These recessive mutants form one large complex complementation group and will be described elsewhere. One-third of the strains were dominant to the wild type for drug resistance. One of these dominant alleles (*TFP1-408*), which was distinct from the recessive locus by genetic analysis and showed a consistent TFP-resistant phenotype, was chosen for further analysis.

***TFP1-408* cells calcium sensitive for growth.** The growth efficiency of mutant and wild-type cells at 26°C was measured by challenging a fixed number of log-phase cells with YPD medium containing various concentrations of calcium and TFP (Fig. 1). When no calcium or other salts were added, wild-type cells were sensitive to 10 μM TFP, whereas mutant cells could grow at concentrations up to 25 μM TFP (Fig. 1A). This window of drug resistance shifted as the calcium concentration was changed (Fig. 1A through E). The wild-type cells became progressively more resistant to the presence of TFP, and the mutant cells appeared to become slightly more resistant to higher TFP concentrations.

When the YPD medium contained a high concentration of added Ca^{2+} (50 mM, Fig. 1E), the growth of wild-type cells was resistant to 20 to 25 μM TFP, and the growth of mutant cells was inhibited in the presence or absence of TFP. The addition of 100 mM KCl, 100 mM NaCl (data not shown), or 50 mM $MgCl_2$ (Fig. 1F) did not alter the growth efficiency of mutant cells to the same extent as the addition of calcium. Mg^{2+} was as effective as Ca^{2+} in rescuing wild-type cells from the inhibitory effects of TFP in the medium (Fig. 1F) (data not shown). The addition of 100 mM KCl or NaCl to YPD medium did not rescue wild-type cells (data not shown). Therefore the susceptibility of wild-type cells to TFP was dependent not only on the concentration of the drug in the media but also on the concentration of Mg^{2+} and Ca^{2+}. Mutant cells were resistant to TFP only within a small concentration range and were sensitive to a high concentration of Ca^{2+} added to YPD medium but not Mg^{2+}, K^+, or Na^+.

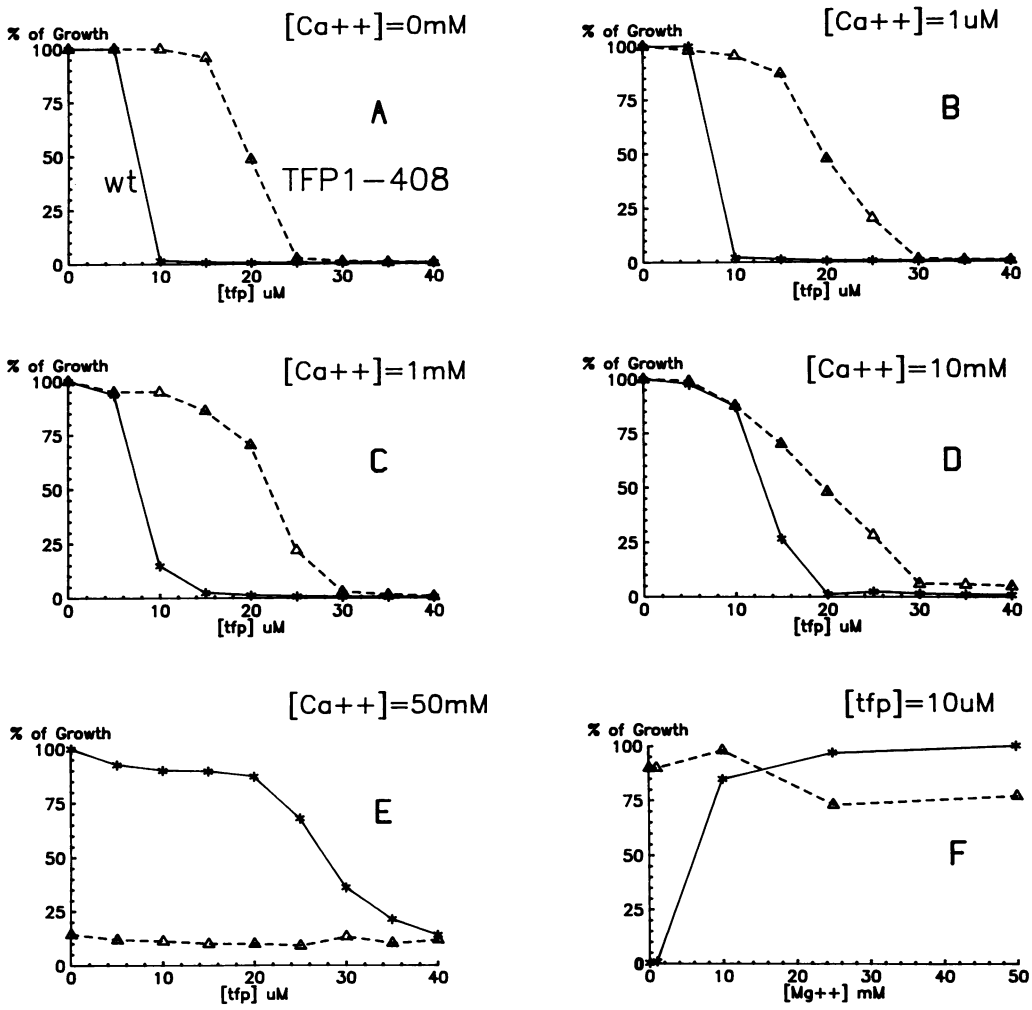

FIG. 1. Growth efficiency test. Equal numbers of wild-type NF147 cells (*) or mutant NF408 (△) cells were seeded into YPD medium plus calcium or other salts, with or without TFP. The efficiency of growth of each cell type is plotted as a function of the TFP concentration with variation in the amount of $CaCl_2$ added in each experiment as indicated in panels A through E. Panel F shows the efficiency of growth of wild-type NF147 cells and mutant NF408 cells in the presence of 10 μM TFP as a function of added $MgCl_2$.

Higher rate of calcium uptake with *TFP1-408* cells compared with wild-type cells. A number of studies have suggested that phenothiazines, especially TFP, stimulate an energy-dependent Ca^{2+} influx in yeast cells at micromolar calcium concentrations (11, 12, 38). The rate of $^{45}Ca^{2+}$ uptake into mutant and wild-type cells was measured; the mutant cells showed a reproducibly higher rate of calcium uptake as compared with wild-type cells measured in parallel in the same experiment (Fig. 2). No uptake was observed when glucose was omitted (data not shown), suggesting that the uptake was energy dependent. The uptake of $^{45}Ca^{2+}$ into mutant and wild-type cells was linear in each experiment during the entire 60-min time course (data not shown).

In a single experiment, the addition of 10 μM TFP and 1 mM $CaCl_2$ caused a 10 to 30% decrease in the rate of $^{45}Ca^{2+}$ influx in both mutant and wild-type cells, relative to cells with no added TFP (data not shown). This result suggests that under approximately physiological calcium concentration conditions (8), TFP inhibits Ca^{2+} influx in both cell types. There was not a simple relationship between Ca^{2+} uptake and the mutation to TFP resistance; that is, the mutation to TFP resistance did not confer TFP-resistant Ca^{2+} uptake.

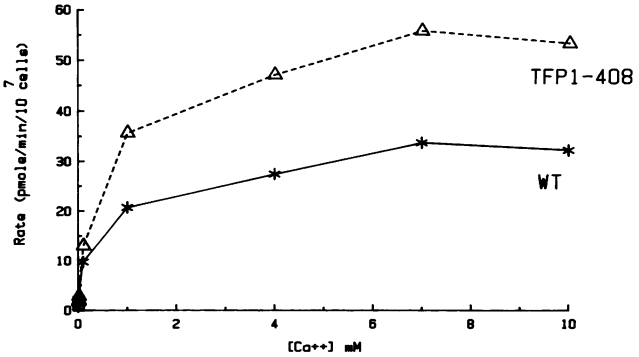

FIG. 2. $^{45}Ca^{2+}$ uptake. The results from individual time course experiments with wild-type NF147 cells (*) and mutant NF408 cells (△) are expressed as the rate of $^{45}Ca^{2+}$ uptake as a function of the $CaCl_2$ concentration in each experiment. Cells harvested and washed after 60 min of uptake did not show any measurable efflux of counts within a single experiment (1 to 60 min).

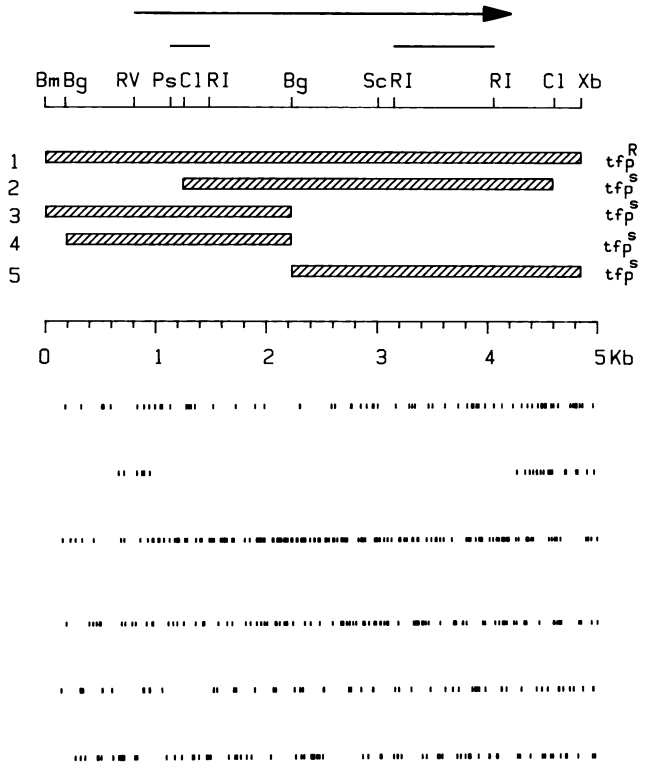

FIG. 3. Molecular analysis of the 5.5-kb *Xba*I genomic restriction fragment. The location of a subset of the restriction enzyme cleavage sites is shown as well as the specific DNA fragments subcloned into YCp50. Restriction enzyme abbreviations: Bm, *Bam*HI; Bg, *Bgl*II; RV, *Eco*RV; Ps, *Pst*I; Cl, *Cla*I; RI, *Eco*RI; Sc, *Sac*II; Xb, *Xba*I. The phenotypes of the resulting URA^+ transformants are shown on the right-hand side. The size scale is indicated in the middle of the figure. The location of nonsense codons in all six reading frames, predicted from the DNA sequence (Fig. 4), is shown in the bottom half of the figure. The direction of transcription of the complementary 3.4-kb poly(A)$^+$ RNA species is indicated, as determined by using strand-specific hybridization probes generated from the single-stranded M13 clones. Two of the restriction fragments used as hybridization probes against poly(A)$^+$ RNA are indicated by lines at the top of the figure.

These data demonstrate that *TFP1-408* cells have two physiological, calcium-related differences from wild-type cells and that the TFP susceptibility of wild-type cells is dependent upon the Ca^{2+} or Mg^{2+} concentration in the medium. These results suggest that the *TFP1-408* mutation affects Ca^{2+} transport through an alteration in the expression or activity of a component of the dynamic ion-exchange network. To further these studies, the *TFP1-408* gene was isolated on the basis of its dominant TFP resistance.

Isolation of the *TFP1-408* gene and determination of its chromosomal location. A library or pool of plasmids containing random fragments of genomic DNA from NF408 cells was made in the plasmid vector YCp50. Purified plasmid DNA was transformed into NF134 cells, and URA^+ transformants were selected. Pooled yeast colonies were plated on TFP-containing media to select for cells containing the dominant TFP resistance gene. Total DNA was made from 12 transformants, and the plasmids were rescued into *E. coli*, selecting for ampicillin resistance. Three different plasmids were recovered with an average insert size of 12 kb, and restriction enzyme digestion revealed a 5.5-kb *Xba*I fragment common to all plasmids (data not shown). This DNA fragment in plasmid vector YCp50 was sufficient to confer TFP resistance to wild-type cells. Smaller DNA fragments were tested by subcloning into plasmid vector YCp50 (Fig. 3). Only the largest DNA fragment of 5 kb (*Bam*HI to *Xba*I) conferred TFP resistance to wild-type cells.

To further localize the coding sequence, several restriction fragments were used as hybridization probes against yeast poly(A)$^+$ RNA. The 5-kb *Bam*HI-to-*Xba*I fragment hybridized to two poly(A)$^+$ RNA species, one of 800 base pairs and a much less abundant 3,400-base-pair mRNA species (data not shown). Several restriction fragments hybridized only to the larger RNA species (indicated at the top of Fig. 3), and an *Eco*RI-*Xba*I restriction fragment (from the right-hand end of the restriction map in Fig. 3) hybridized only to the smaller RNA. This suggested that the larger RNA species coded for the TFP resistance gene, since DNA fragments which contained the cloned region complementary to the small RNA did not confer TFP resistance (Fig. 3).

Hybridization of the 1.8-kb *Eco*RI internal restriction fragment to separated yeast chromosomes showed that this gene was located on chromosome IV (Fig. 4). Two controls were used to positively identify chromosome IV. Hybridization probes for cloned genes (*HO*, *TRP1*, *CDC7*, *TRT1*) mapping to chromosome IV (26, 28) were used in parallel hybridizations. In addition a strain YNN311 containing a II: IV translocation was used to identify the left and right arms of chromosome IV. The two known markers from the left or short arm of chromosome IV (*CDC7* in Fig. 4A, *HO* in Fig. 4B) hybridized to wild-type and translocation strain chromosomes in a pattern similar to that with the *TFP1* probe (Fig. 4C). The two known markers for the right or long arm of chromosome IV (*TRP1* in Fig. 4D; *TRT1* in Fig. 4E) hybridized to the wild-type chromosomes exactly as did the other probes and, as expected, hybridized to a more slowly migrating chromosome in the translocation strain (Fasullo, thesis). This result localizes the *TFP1* locus to chromosome IV and more specifically to the left or short arm.

The wild-type *TFP1* gene was isolated from a lambda phage library of NF134 DNA cloned in vector EMBL3B (18). The corresponding wild-type 5-kb *Bam*HI-to-*Xba*I restriction fragment (Fig. 3) was ligated into YCp50, and the

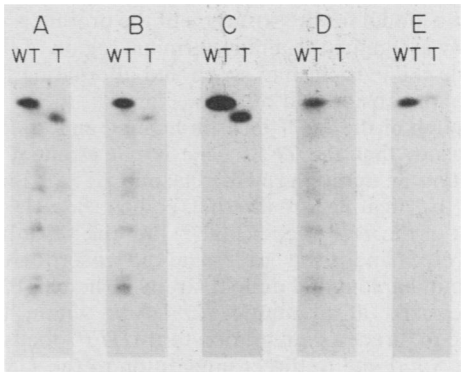

FIG. 4. Mapping of the *TFP1* locus to chromosome IV. Spheroplasts from wild-type (NF147) and translocation (YNN311) strains were cast in agarose and loaded on alternating lanes of a contour-clamped homogeneous electric field gel (5). The chromosome gel was transferred to a nylon membrane and divided into five identical filters, each containing one lane of wild-type (WT) chromosomes and one lane of the translocation (T) strain chromosomes. Hybridization was with the following: A, *CDC7* gene (marker for left arm of chromosome IV); B, *HO* gene (left arm); C, *TFP1* gene (*Eco*RI 1.8-kb fragment, Fig. 3); D, *TRP1* gene (right arm); and E, *TRT1* (histone *H2A* and *H2B* genes) (right arm).

plasmid DNA was transformed into NF134 cells. The resulting URA$^+$ transformants were still susceptible to TFP, demonstrating that two copies of the wild-type sequence was not sufficient to confer TFP resistance to wild-type cells. The wild-type gene and the dominant TFP resistance gene were ligated into the yeast plasmid vector YEp24, a high-copy-number plasmid with a URA3$^+$ selectable marker. These plasmids were used to transform NF147, and 0.1 to 1 transformant per μg of plasmid DNA was found for both constructions, as opposed to 800 transformants per μg with vector YEp24 DNA. This low frequency of transformation for cloned genes on YEp24 or other high-copy-number yeast plasmid vectors has been seen before in cytoskeleton-related genes such as the actin gene (15) and suggests that the overexpression of the *TFP1* gene product is lethal to the haploid cells.

DNA sequence of the *TFP1* gene predicts a large protein of 1,031 amino acids. The nucleotide sequence of the 5-kb *Bam*HI-to-*Xba*I fragment was determined (Fig. 5). There was only one large open reading frame in all six possible reading frames (Fig. 3). The DNA sequence of the large open reading frame predicted a protein of 1,031 amino acids (Fig. 5). There was no yeast consensus splice sequence (15), which indicates that the mRNA for this gene is not spliced and therefore that the first methionine codon in the open reading frame is likely to code for the start of translation. In the 5′-upstream portion of the sequence there was a poly(dT)- and poly(dA)-rich region (nucleotides 680 through 728) and a TATAA sequence (nucleotides 886 through 890).

***TFP1-408* gene product homology with the β-subunit of F_0F_1 ATP synthase and possible transmembrane domains.** A sequence homology search (21) of the predicted amino acid sequence of the *TFP1-408* gene product against known protein sequences revealed a 37% identity of one region of the *TFP1-408* gene with the β-subunit of F_0F_1 ATP synthase (Fig. 6). This region of the β-subunit of F_0F_1 ATP synthase is thought to interact with the α-subunit to form part of the ATP-binding domain (14).

The hydrophobicity profile (13, 20) of the predicted amino acid sequence of the *TFP1-408* gene product displayed several potential hydrophobic domains sufficient in length to span the cell membrane (Fig. 7A and B, regions 1 through 7). A possible model for the structure of the protein is proposed, arbitrarily assigning the amino-terminal region of the protein to outside the cytoplasmic space and alternating the hydrophilic regions inside and outside (Fig. 7C).

Disruption of the *TFP1* locus in haploid and diploid strains demonstrates that the *TFP1* gene is not essential for spore germination or mitotic growth. Plasmid pTFP1-18 was constructed by ligating an internal coding *Eco*RI restriction fragment of the *TFP1* gene (Fig. 3) into the yeast integrating vector YIp5 and used to create an insertion-disruption mutation in haploid and diploid strains. The pTFP1-18 DNA was linearized at a unique *Kpn*I site within the *TFP1* sequence to direct its integration to the *TFP1* locus (36) or at a unique *Sma*I site to direct integration to the *URA3* locus. The transformation frequency of *Kpn*I-cut pTFP1-18 DNA was 400 URA$^+$ transformants per μg of DNA into haploid strain NF147 and 930 transformants per μg of DNA into a diploid strain (NF147 × NF134) homozygous for the *ura3-52* mutation. The transformation of *Sma*I-cut plasmid DNA was 130 URA$^+$ transformants per μg of DNA in the haploid strain and 180 transformants per μg of DNA in the diploid strain.

There was a twofold-lower efficiency of transformation into haploid versus diploid cells at the *TFP1* locus, and the efficiency of transformation into cells at the *URA3* locus was the same but lower overall in haploid and diploid cells. The lower efficiency of integrative transformation at the *ura3-52* locus is due to the presence of a TY element in the coding sequence of the *URA3* gene (35). The twofold difference between integration of pTFP1-18 at the *TFP1* locus in haploid versus diploid cells is probably not significant, since the diploid cells have two equally good target alleles. The integration of the construction at the *TFP1* locus was confirmed by gel transfer-hybridization analysis (Fig. 8). These data suggest that the *TFP1* gene is not essential for mitotic growth.

TABLE 1. Tetrad viability from *TFP1* disruption heterozygotes

Type of disruption	Spore viability in tetrads					Total no. of tetrads examined
	$4^+:0^0$	$3^+:1^0$	$2^+:2^0$	$1^+:3^0$	$0^+:4^0$	
Insertion	7	12	9	7	5	40
Replacement	7	13	9	3	5	37
Integration at *URA3* locus	8	5	1	5	1	20

A diploid strain (NF134 × NF408) homozygous for the *ura3-52* mutation and heterozygous at the TFP1 locus (*tfp1*$^+$/*TFP1-408*) was transformed with *Kpn*I-cut pTFP1-18 DNA. Of 144 URA$^+$ transformants tested, 68 (47%) were TFP susceptible and 76 (53%) were TFP resistant. This is the expected result if the plasmid integrated randomly into either the dominant *TFP1-408* allele, creating a TFP-susceptible transformant or into the wild-type TFP-susceptible allele, where the resulting transformant remains TFP resistant. Integration of *Sma*I-cut pTFP1-18 DNA at the *URA3* locus yielded only URA$^+$ TFP-resistant transformants (18 of 18).

Two URA$^+$ TFP-susceptible and two URA$^+$ TFP-resistant diploids were sporulated, and 40 tetrads from the four independent diploids were dissected. Eighty-nine spores grew into visible colonies for a 56% viability (Table 1). Of these surviving spores, 40 (45%) were URA$^+$. The URA$^+$ spores germinated more slowly than did the ura$^-$ spores. Tetrads were dissected from control diploids, where the plasmid integrated at the *URA3* locus and a similar spore viability was found (Table 1). The spore inviability seen in these experiments is not due to the construction at the *TFP1* locus.

Genomic DNA was prepared from one of the TFP-resistant URA$^+$ transformants, from one of the TFP-susceptible URA$^+$ transformants, and from the germinated spores of a complete tetrad from each of these diploid transformants. The DNA preparations were digested with restriction enzyme *Xba*I, and gel transfer-hybridization analysis was performed with the 1.8-kb *Eco*RI fragment of the *TFP1* gene as the probe. The wild-type 5.5-kb *Xba*I fragment was present in the untransformed diploid (Fig. 8, lane 1), and insertion of the disruption construction into one or the other alleles of the *TFP1* locus increased the size of the *Xba*I fragment to 12.8 kb (Fig. 8, lanes 2 and 7). The ura$^-$ spores from both diploid transformants had the wild-type 5.5-kb *Xba*I fragment (Fig. 8, lanes 5, 6, 8, and 9), and the URA$^+$ spores had the disruption 12.8-kb fragment (Fig. 8, lanes 3, 4, 10, and 11). The results of these experiments show that the *TFP1* gene is not required for spore germination or mitotic growth.

A similar series of experiments was performed transforming a diploid strain with a null allele replacement-disruption construction. The null allele construction replaces the coding region of the *TFP1* gene with the *URA3*$^+$ gene. The null

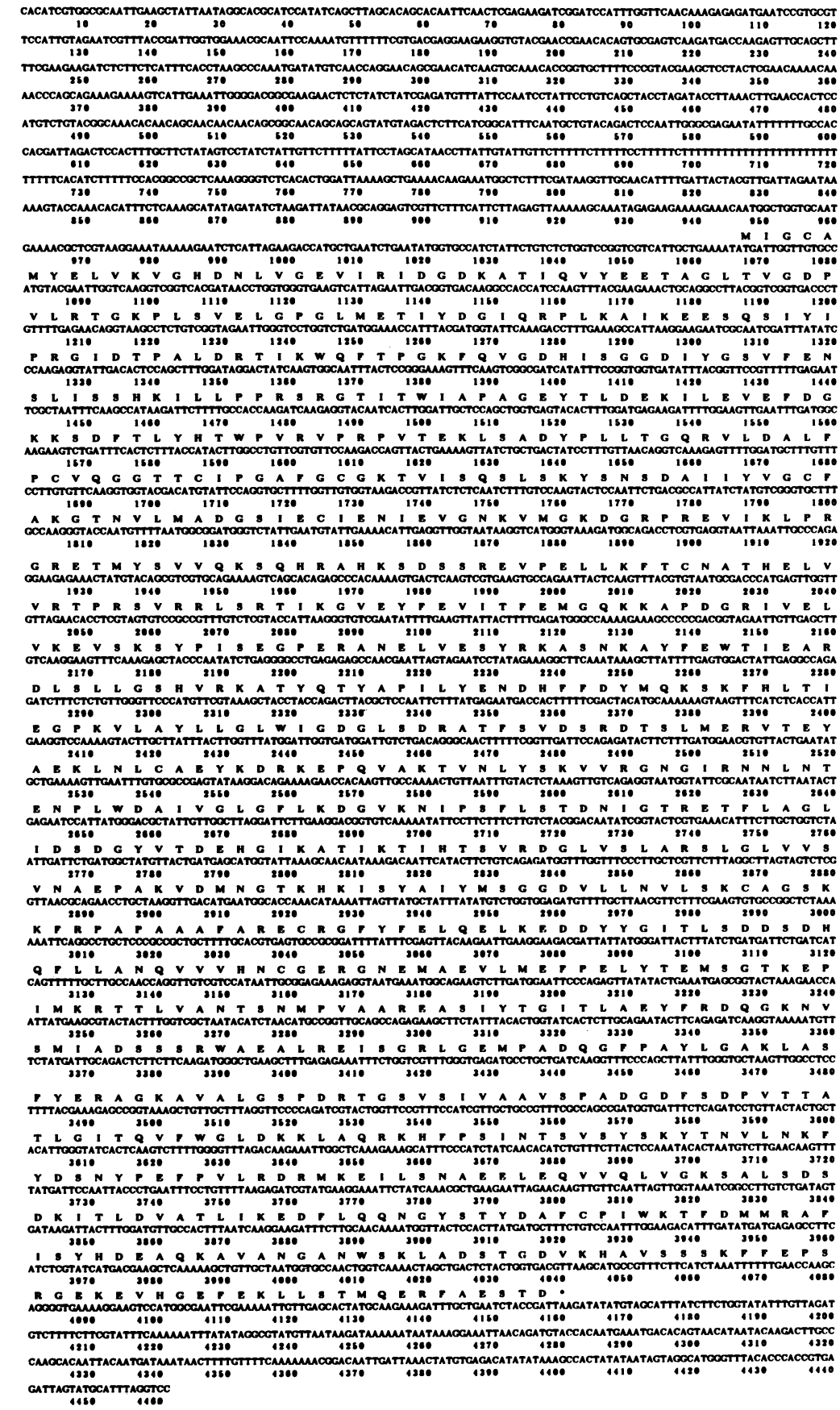

FIG. 5. DNA sequence of the *TFP1-408* gene. The predicted amino acid sequence is shown in the one-letter amino acid code.

```
TFP1-408                    791 L V A N T S N M P V A A R E A S I Y T G I T L A E Y F R D Q - G K N V S M I A D S S S R N A E
Yeast Mit. ATPase ß          56 L V F G Q M N E P P E A R A R V A L T G L T I A E Y F R D E E G Q D V L L - Y D N I F R F T Q
Bovine Mit. ATPase ß        217 L V Y G Q M N Q P P G A R A R V A L T G L T V A E Y F R D Q E G Q D V L L F I D N I F R F T Q
E. Coli ATPase ß            205 L V Y G Q M N E P P G N R L R V A L T G L T M A E K F R D E G R D V L L F - V D N I Y R Y T L
Barley Chl. ATPase ß        234 L V Y G Q M N E P P G A R M R V G L T A L T M A E Y F R D V N K Q D V L L F I D D I F R F V Q
Common Tob. Chl. ATPase ß   234 L V Y G Q M N E P P G A R M R V G L T A L T M A E Y F R D V N E Q D V L L F I D N I F R F V Q
Maize Chl. ATPase ß         234 L V Y G Q M N E P P G A R M R V G L T A L T M A E Y F R D V N K Q D V L L F I D N I F R F V Q

TFP1-408                    A L R E I S G R L G E M P A D Q G F P A Y L G A K L A S F Y E R 868
Yeast Mit. ATPase ß         A G S E V S A L L G R I P S A V G Y Q P T L A T D M G L L Q E R 133
Bovine Mit. ATPase ß        A G S E V S A L L G R I P S A V G Y Q P T L A T N M G T M Q E R 295
E. Coli ATPase ß            A G T E V S A L L G R M P S A V G Y Q P T L A E E M G V L Q E R 282
Barley Chl. ATPase ß        A G S E V S A L L G R M P S A V G Y Q P T L S T E M G S L Q E R 312
Common tob. Chl. ATPase ß   A G S E V S A L L G R M P S A V G Y Q P T L S T E M G S L Q E R 312
Maize chl. ATPase ß         A G S E V S A L L G R M P S A V G Y Q P T L S T E M G S L Q E R 312
```

FIG. 6. *TFP1* has homology with the β-subunit of F_0F_1 ATP synthase. Identical amino acids are boxed. The position of this region within each protein sequence is indicated by the amino acid numbers flanking the sequence. The amino acid sequence of the β-subunit of the ATPase complex is highly conserved among different organisms (19, 37, 39, 41, 46, 51).

allele plasmid pTFP1-13 was digested with *Xba*I to direct the integration of the construction to the *TFP1* locus, where a recombination event involving a double crossover (36) replaced one of the *TFP1* alleles with the *URA3*$^+$ gene. The tetrads resulting from the sporulation of three independent URA$^+$ diploid transformants were dissected and analyzed (Table 1). The results are identical to those in the previous series of experiments. There was a 59% (88 of 148) spore viability, and 53% (47 of 88) of the surviving spores were URA$^+$. A gel transfer-hybridization analysis confirmed the presence of the null construction (2.3-kb *Xba*I fragment) in the independent URA$^+$ diploid transformants and in the URA$^+$ spores from two of the independent diploid transformants (data not shown). In addition, all of the ura$^-$ spores contained the wild type-sized 5.5-kb *Xba*I fragments, as did the untransformed diploid strain and the URA$^+$ transformants. This result was found from tetrads with two, three, or four surviving spores. URA$^+$ spores from a third unusual diploid transformant with only a 25% spore survival contained the wild-type 5.5-kb *Xba*I fragment at the *TFP1* locus and had undergone some type of gene conversion event converting the 11.6-kb *Bam*HI fragment of the *ura3-52* allele (35) to the 5.5-kb wild-type fragment size (data not shown). The data from both the insertion-disruption and the null allele replacement constructions demonstrate that the *TFP1* gene is not essential for spore germination and mitotic growth.

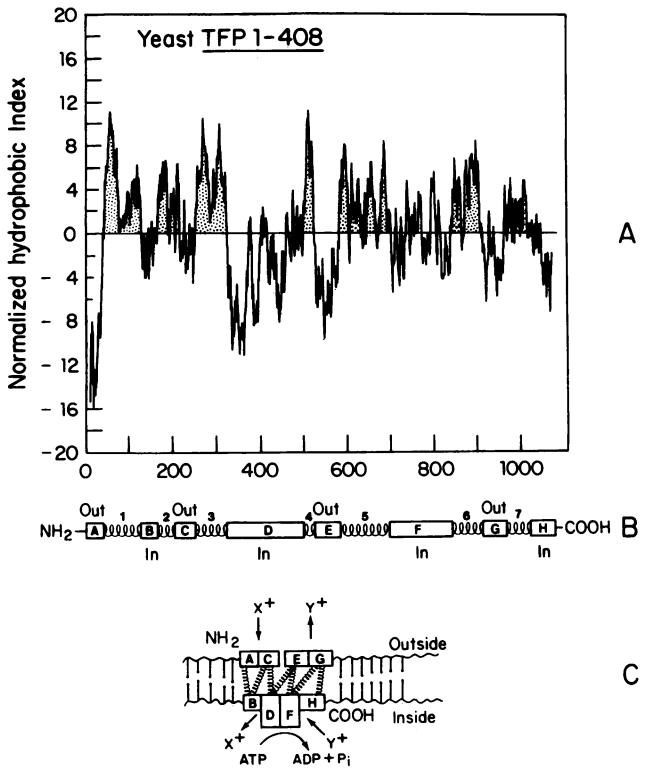

FIG. 7. Hydrophobicity profile of the *TFP1* gene product. The predicted amino acid sequence of the large open reading frame was analyzed for relative hydrophobic and hydrophilic domains (13, 20) (A). A positive value indicates increasing hydrophobicity. A hypothetical model for the structure of the *TFP1* gene product is shown (B and C). Regions 1 through 7 are hydrophobic and encode potential transmembrane segments. Regions A through H are hydrophilic and are arbitrarily assigned as inside or outside, beginning with the amino-terminal end of the protein sequence.

DISCUSSION

The gene we isolated has several interesting phenotypic and molecular features. Cells containing the *TFP1-408* allele

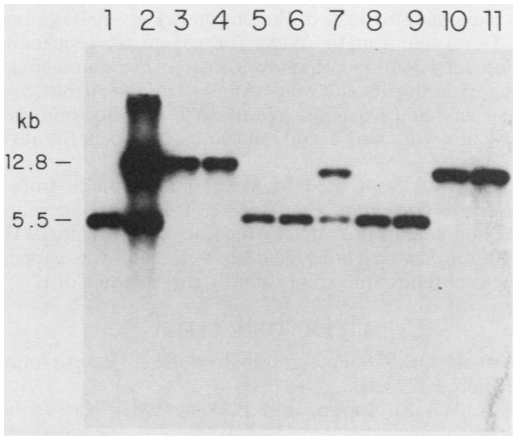

FIG. 8. Gel-transfer hybridization of total yeast DNA from strains transformed with *TFP1::URA3*(YIp5) insertion-disruption construction. Total yeast DNA was prepared from the original ura$^-$ TFP-resistant diploid (NF134 × NF408) (lane 1), one URA$^+$ TFP-resistant diploid transformant (lane 2), one URA$^+$ TFP-susceptible diploid transformant (lane 7), and from the four spores of a tetrad from each of the diploid transformants (lanes 3 through 6 and 8 through 11). The DNA samples were digested with *Xba*I and separated on an agarose gel. The DNA gel was transferred to a nylon membrane and analyzed with a *TFP1* probe (*Eco*RI 1.8-kb fragment [Fig. 3]). The normal *TFP1* locus is on a 5.5-kb *Xba*I fragment, and the insertion-disruption allele is on a 12.8-kb fragment.

were resistant to TFP (10 to 15 μM, YPD medium), showed calcium-sensitive growth, and had a higher rate of calcium uptake relative to wild-type parental cells. The DNA sequence of the *TFP1-408* allele revealed a large open reading frame whose translation predicts a large protein of 1,031 amino acids, with homology to ATP synthase and possible transmembrane domains. A chromosome hybridization experiment localized the *TFP1* gene to chromosome IV, distinguishing it from the pleiotropic drug resistance locus *PDR1* located on chromosome VII (26). The *TFP1* gene was not required for spore germination or mitotic growth, but overexpression of the *TFP1* gene from a high-copy-number plasmid vector was lethal to haploid cells.

Calcium metabolism and calcium-sensitive mutants in *S. cerevisiae*. Yeast cells require calcium for growth and presumably transport calcium across the plasma membrane via specific channels or exchangers as found in other cells (3, 8). Once a specific channel or transporter is activated in the plasma or organelle membrane, Ca^{2+} enters the cytoplasm, flowing down the large concentration gradient that exists between the intracellular (10^{-7} M) and the extracellular (1 mM) space. The localized influx of Ca^{2+} into the cytoplasm must be matched by efflux into the extracellular space or into an organelle compartment. The major calcium storage organelle in yeast cells is presumably the vacuole (29), although significant stores probably exist in the mitochondria and endoplasmic reticulum (8). The efflux from the cytoplasmic compartment is achieved by activation of membrane-associated Ca^{2+}-ATPases (3) or possibly by analogy with higher cells, Na^+-driven calcium antiports. The *TFP1-408* mutant cells showed a higher rate of calcium uptake relative to wild-type parental cells and calcium-sensitive growth. The rate of calcium uptake saturates in mutant and wild-type cells at the same calcium concentration (approximately 7 mM Ca^{2+}), but the mutant cells show a higher maximal velocity. These kinetic data are consistent with mutant and wild-type cells having the same affinity for calcium ions and a higher activity of the transport process in the mutant cells. Although the rate of calcium uptake saturates in the mutant cells at 7 mM, the cells do not show calcium-sensitive growth until 50 mM $CaCl_2$ is added to YPD medium. The measurement of calcium uptake is exclusively a measure of uptake, as we could not demonstrate efflux in $^{45}Ca^{2+}$-loaded cells. The growth efficiency test reflects general cellular metabolism and presumably the ability of the cells to internally regulate the higher rate of calcium influx against a large extracellular gradient.

The *TFP1* gene product may be a subunit of one of these calcium-specific pumps or channels or, more likely, a proton or other ion pump whose activity affects the function of plasma membrane calcium channels or transporters. A calcium transport activity has been demonstrated and partially purified from isolated yeast vacuole membranes (29), but little is known about plasma membrane calcium transport or intracellular calcium mobilization in yeast cells.

Calcium-sensitive mutants (31, 32) and TFP-resistant pseudorevertants of a calcium-dependent mutant (30) of *S. cerevisiae* have been reported. The calcium-dependent mutant *cal 1-1* is temperature sensitive and shows a cell cycle stage-specific arrest at the restrictive temperature. The TFP-resistant pseudorevertant of this mutant is recessive to the wild-type and showed TFP-dependent growth at 37°C. These mutants appear to be different from the *TFP1-408* mutant described here, although it may be allelic with one of the 18 complementation groups of calcium-sensitive mutants, some of which show higher rates of Ca^{2+} uptake (32).

Relationship between TFP resistance and the *TFP1* gene product. Eilam (10–12) observed that the effect of TFP on yeast cells in the presence of 1 μM Ca^{2+} is to stimulate an influx of Ca^{2+} into yeast cells, coupled with an efflux of K^+. A model was proposed that TFP activates energy-dependent K^+ extrusion pumps, which lead to increased membrane potential (12). Under these conditions the influx of Ca^{2+} is a secondary event caused by the increased membrane potential. The stimulatory effect of TFP on Ca^{2+} uptake was abolished at 1 mM $CaCl_2$ or when 10 to 100 mM KCl, 100 mM NaCl, or 1 mM $MgCl_2$ was included in the incubation medium. These results support our observations that the effect of TFP on cells is dependent upon the ionic composition of the media and the idea that TFP may affect membrane potential.

TFP is a very hydrophobic drug and may intercalate into membranous structures. There may not be a specific protein target for the drug per se, as suggested in earlier work on a macrophage cell line (47), or in numerous studies where its effects are assumed to be due to an inhibition of calmodulin, but rather the presence of TFP in the membrane may create a general disturbance in the electrochemical gradients across the affected membrane, possibly through a lowering of membrane fluidity. This is consistent with its pharmacological properties as well as its effect on yeast cells. A generalized hydrophobic effect model does not predict calcium specificity, unless a hypothesis is made that calcium transport-mobilization processes are especially sensitive to membrane potential disturbances or that TFP has an affinity for electrogenic membranes where active calcium transport contributes to the potential difference.

Our TFP-resistant mutant has a higher rate of Ca^{2+} uptake than the wild type and cannot grow efficiently in the presence of 50 mM Ca^{2+}. In one experiment the addition of TFP inhibited the rate of Ca^{2+} uptake in mutant and wild-type cells. Therefore the effect of TFP on yeast cells under more physiological conditions (8) may be to inhibit Ca^{2+} uptake

directly or to lower the membrane potential through inhibition of a membrane ATPase. The higher rate of Ca^{2+} uptake in mutant cells appears to be due to a constitutively higher activity of the Ca^{2+} transport system. By one model the *TFP1-408* gene product might code for a protein directly involved in Ca^{2+} translocation across the membrane. The higher activity of the mutant protein would be such that high external Ca^{2+} concentration proves lethal to mutant cells. Alternatively, the increased rate of Ca^{2+} influx in mutant cells may result from an increased membrane potential in mutant cells due to the higher activity of an energy-dependent Na^+ or K^+ efflux pump. The increased membrane potential would allow voltage-gated calcium channels to open more frequently or remain open longer. The physiological studies on the mutant and wild-type cells are more consistent with the second model.

Because of its size, amino acid homology with ATP synthases, and predicted transmembrane regions, the *TFP1* gene product is likely to be some type of proton ATPase associated with a membrane involved in calcium transport (1, 14). Precisely which ions are transported or exchanged is not known. There is no direct evidence to date that the *TFP1-408* gene product is a target for TFP binding in vivo.

The *TFP1* gene is not essential for spore germination and mitotic growth by construction and analysis of disruption mutants. Therefore the *TFP1* gene product activity in the haploid cells can be replaced by some other gene product. Hybridization of DNA fragments of the *TFP1* locus to total yeast DNA at a high stringency of hybridization does not reveal any closely related genes (Fig. 4C and 8). Growth of the disruption mutants on different media or under temperature conditions has not been investigated, nor has sensitivity of the mutants to TFP. Overexpression of the gene on a high-copy-number yeast vector is lethal to haploid cells, which will allow the isolation of more mutants of the *TFP1* gene and identification of second-site suppressor of the overexpression. Once genes encoding potential interacting gene products have been isolated, disruptions of these genes will be tested in combination with the *TFP1* disruption mutations.

ATPases and ion exchangers are important cellular regulators. There are several classes of membrane-bound ATPases that have been described in the biochemical literature (1, 3, 9, 14, 34). These ion pumps contribute to the plasma membrane electrochemical gradient, control cell volume, and can participate in the active transport of amino acids and sugars. The mechanism and activity of these ion pumps is under investigation in numerous systems (34, 49), including *S. cerevisiae*. The gene coding for the major yeast plasma membrane ATPase (*PMA1*) has been isolated recently (44) and is different from *TFP1*, yet shares certain features such as size, predicted transmembrane domains, and a poly(T)-, poly(A)-rich DNA sequence motif in the 5′-upstream region. The activity and function of proton ATPases are of special interest, since these enzymes appear to be responsible for acidification of cellular compartments and generation of transmembrane electrical potentials (1). The regulation of the activity of such ion pumps may contribute to intracellular traffic and organelle function, because local metabolic activity and protein targeting may be influenced by changes in the different electrochemical potentials across the different membranes which enclose cellular compartments.

ACKNOWLEDGMENTS

We thank Wilbur E. Latshaw of Smith Kline and French for the gift of trifluoperazine, Michael Fasullo for the translocation strain, William Holloman for loan of the chromosome separation gel, and Thambi Dorai and Lu-Hai Wang for advice on sequencing. We thank Hannah Klein and Rodney Rothstein for comments on the disruption experiments and Mary Ann Osley and Arthur Lustig for advice, strains, and plasmids. We thank David Botstein, in whose laboratory this work was begun, and Frank Solomon for advice and support.

This work was supported by development funds from Public Health Service core grant CA 08748-20 from the National Cancer Institute and by funds provided by the Society of Memorial Hospital and the Milton Schamach Foundation. C.K. Shih was supported by a postdoctoral fellowship sponsored by the Exxon Corp.

LITERATURE CITED

1. **Al-Awqati, Q.** 1986. Proton-translocating ATPases. Annu. Rev. Cell Biol. **2**:179–200.
2. **Barnes, W., M. Bevan, and P. Son.** 1983. Kilo-sequencing: creation of an ordered nest of asymmetric deletions across a large target sequence carried on phage M13. Methods Enzymol. **101**:98–122.
3. **Carafoli, E.** 1984. Calcium-transporting system of plasma membranes, with special attention to their regulation. Adv. Cyclic Nucleotide Res. **17**:543–550.
4. **Carle, G. F., and M. V. Olsen.** 1985. An electrophoretic karyotype for yeast. Proc. Natl. Acad. Sci. USA **82**:3756–3760.
5. **Chu, G., D. Vollrath, and R. W. Davis.** 1986. Separation of large DNA molecule by contour-clamped homogeneous electric fields. Science **234**:1582–1585.
6. **Dale, R., B. McClure, and J. Houchins.** 1985. A rapid single-stranded cloning strategy for producing a sequential series of overlapping clones for use in DNA sequencing: application to the sequencing the corn mitochondrial 18S rDNA. Plasmid **13**: 13–40.
7. **Davis, R., D. Botstein, and J. R. Roth.** 1980. Advanced bacterial genetics. Cold Spring Harbor Laboratory, Cold Spring Harbor, N.Y.
8. **Davis, T., and J. Thorner.** 1986. Calmodulin and other calcium-binding proteins in yeast, p. 477–503. *In* J. Hicks (ed.), Yeast cell biology. Alan R. Liss, Inc., New York.
9. **De Meis, L., and A. Vianna.** 1979. Energy conversion by the Ca^{++}-dependent ATPase of the sarcoplasmic reticulum. Annu. Rev. Biochem. **48**:275–292.
10. **Eilam, Y.** 1982. The effect of monovalent cations on calcium efflux in yeasts. Biochim. Biophys. Acta **687**:8–12.
11. **Eilam, Y.** 1983. Membrane effects of phenothiazines in yeasts. I. Stimulation of calcium and potassium fluxes. Biochim. Biophys. Acta **733**:242–248.
12. **Eilam, Y.** 1984. Effects of phenothiazines on inhibition of plasma membrane ATPase and hyperpolarization of cell membranes in the yeast *S. cerevisiae*. Biochim. Biophys. Acta **769**: 601–610.
13. **Eisenberg, D. A.** 1984. Three-dimensional structure of membrane and surface proteins. Annu. Rev. Biochem. **53**:595–623.
14. **Futai, M., and H. Kanazawa.** 1983. Structure and functions of the proton-translocating adenosine triphosphatase (F_0F_1): biological and molecular biological approaches. Microbiol. Rev. **47**:285–312.
15. **Gallwitz, D.** 1982. Construction of a yeast actin gene intron deletion mutant that is defective in splicing and leads to the accumulation of the precursor RNA in transformed yeast cells. Proc. Natl. Acad. Sci. USA **79**:3493–3497.
16. **Holm, C., D. M. Meeks-Wagner, W. L. Fangman, and D. Botstein.** 1986. A rapid, efficient method for isolating DNA from yeast. Gene **42**:169–173.
17. **Ito, H., Y. Fukuda, K. Murata, and A. Kimura.** 1983. Transformation of *Saccharomyces cerevisiae* with lithium ions. J. Bacteriol. **153**:163–168.
18. **Kaiser, K., and N. E. Murray.** 1985. The use of phage lambda replacement vectors in the construction of representative genomic DNA libraries, p. 1–47. *In* D. M. Glover (ed.), DNA cloning, vol. 1. IRL Press, Oxford.
19. **Krebbers, E. T., I. M. Larrinua, L. McIntosh, and L. Bogorad.** 1982. The maize chloroplast genes for the beta and epsilon

subunits of the photosynthetic coupling factor CF_1 are fused. Nucleic Acids Res. **10**:4985–5002.
20. **Kyte, J., and R. F. Doolittle.** 1982. A simple method for displaying the hydropathic character of a protein. J. Mol. Biol. **157**:105–132.
21. **Lipman, D. J., and W. R. Pearson.** 1985. Rapid and sensitive protein similarity searches. Science **227**:1435–1441.
22. **Maniatis, T., E. F. Fritsch, and J. Sambrook.** 1982. Molecular cloning: a laboratory manual. Cold Spring Harbor Laboratory, Cold Spring Harbor, N.Y.
23. **Messing, J., R. Crea, and P. H. Seeburg.** 1981. A system for shotgun DNA sequencing. Nucleic Acids Res. **9**:309–321.
24. **Miller, R. J., and C. R. Hiley.** 1974. Anti-muscarinic properties of neuroleptics and drug-induced parkinsonism. Nature (London) **248**:596–597.
25. **Mori, T., Y. Takai, R. Minakuchi, B. Yu, and Y. Nishizuka.** 1980. Inhibitory action of chlorpromazine, dibucaine, and other phospholipid-interacting drugs on calcium-activated phospholipid-dependent protein kinase C. J. Biol. Chem. **255**:8378–8380.
26. **Mortimer, R. K., and D. Schild.** 1985. Genetic map of *Saccharomyces cerevisiae*, edition 9. Microbiol. Rev. **49**:181–212.
27. **Neff, N., J. Thomas, P. Grisafi, and D. Botstein.** 1983. Isolation of the β-tubulin gene of *S. cerevisiae* and demonstration of its essential function *in vivo*. Cell **33**:211–219.
28. **Norris, D., and M. A. Osley.** 1987. The two gene pairs encoding H2A and H2B play different roles in the *Saccharomyces cerevisiae* life cycle. Mol. Cell. Biol. **7**:3473–3481.
29. **Ohsumi, Y., and Y. Anraku.** 1985. Calcium transport driven by a proton motive force in vacuolar membrane vesicles of *S. cerevisiae*. J. Biol. Chem. **258**:5614–5619.
30. **Ohya, Y., Y. Ohsumi, and Y. Anraku.** 1984. Genetic study of the role of calcium ions in the cell division cycle of *S. cerevisiae*: a calcium-dependent mutant and its trifluoperazine-dependent pseudo-revertants. Mol. Gen. Genet. **193**:389–406.
31. **Ohya, Y., S. Miyamoto, Y. Ohsumi, and Y. Anraku.** 1986. Calcium-sensitive *cls4* mutant of *S. cerevisiae* with a defect in bud formation. J. Bacteriol. **165**:28–33.
32. **Ohya, Y., Y. Ohsumi, and Y. Anraku.** 1986. Isolation and characterization of Ca^{++}-sensitive mutants of *S. cerevisiae*. J. Gen. Microbiol. **132**:979–988.
33. **Post, A., R. J. Warren, and J. E. Zarembo.** 1980. Trifluoperazine hydrochloride. Anal. Profiles Drug Substances **9**:543–579.
34. **Racker, E.** 1976. Reconstitution and mechanism of action of ion pumps, p. 88–89. *In* A new look at mechanisms in bioenergetics. Academic Press, Inc., New York.
35. **Rose, M., and F. Winston.** 1984. Identification of a Ty insertion within the coding sequence of the *S. cerevisiae URA3* gene. Mol. Gen. Genet. **193**:557–560.
36. **Rothstein, R.** 1983. One step gene disruption in yeast. Methods Enzymol. **101**:202–211.
37. **Runswick, M., and J. E. Walker.** 1983. The amino acid sequence of the beta subunit of the ATP synthase from bovine heart mitochondria. J. Biol. Chem. **258**:3081–3089.
38. **Saavedra-Molina, A., R. Villalobos, and M. Borbolla.** 1983. Calcium uptake during the cell cycle of *S. cerevisiae*. FEBS Lett. **160**:195–197.
39. **Saltzgaber-Muller, J., S. Kunapuli, and M. Douglas.** 1983. Nuclear genes coding the yeast mitochondrial adenosine triphosphatase complex. J. Biol. Chem. **258**:11465–11470.
40. **Sanger, F., S. Nicklen, and A. Coulson.** 1977. DNA sequencing with chain termination inhibitors. Proc. Natl. Acad. Sci. USA **74**:5463–5467.
41. **Saraste, M., N. J. Gay, A. Eberle, M. J. Runswick, and J. E. Walker.** 1981. The *atp* operon: nucleotide sequence of the genes for the gamma, beta, and epsilon subunits of *E. coli* ATP synthase. Nucleic Acids Res. **9**:5287–5296.
42. **Seeman, P.** 1977. Anti-schizophrenic drugs: membrane receptor site of action. Biochem. Pharmacol. **26**:1741–1748.
43. **Segev, N., and D. Botstein.** 1987. The *ras*-like yeast *YPT1* gene is itself essential for growth, sporulation and starvation response. Mol. Cell. Biol. **7**:2367–2377.
44. **Serrano, R., M. Kielland-Brandt, and G. R. Fink.** 1986. Yeast plasma membrane ATPase is essential for growth and has homology with (Na^+, K^+), K^+, and Ca^{++}-ATPases. Nature (London) **319**:689–693.
45. **Sherman, F., G. R. Fink, and J. Hicks.** 1986. Methods in yeast genetics. Cold Spring Harbor Laboratory, Cold Spring Harbor, N.Y.
46. **Shinozaki, K., H. Deno, A. Kato, and M. Sugiura.** 1983. Overlap and cotranscription of the genes for the beta and epsilon subunits of tobacco chloroplast ATPase. Gene **24**:147–155.
47. **Speaker, M., S. Orlow, T. Sturgill, and O. Rosen.** 1983. Characterization of a calmodulin-binding protein that is deficient in trifluoperazine-resistant variants of the macrophage-like cell line J774. Proc. Natl. Acad. Sci. USA **80**:329–333.
48. **Synder, S., D. Greenberg, and H. Yamamura.** 1974. Antischizophrenic drugs and brain cholinergic receptors. Affinity for muscarinic sites predicts extrapyramidal effects. J. Psychiatr. Res. **11**:91–98.
49. **Tanford, C.** 1983. Mechanism of free energy coupling in active transport. Annu. Rev. Biochem. **52**:379–409.
50. **Weiss, B., and R. Levin.** 1978. Mechanism for selectively inhibiting the activation of cyclic nucleotide phosphodiesterase and adenylate cyclase by anti-psychotic agents. Adv. Cyclic Nucleotide Res. **9**:285–303.
51. **Zurawski, G., and M. T. Clegg.** 1984. The barley chloroplast DNA *aptBE*, *trnM2* and *trnV1* loci. Nucleic Acids Res. **12**:2549–2558.